

1 Introduction

1.1 Simulated Annealing

The LAMMPS molecular dynamics code allows for massively parallel simulations with billions of atoms[1]. However, as with all molecular dynamics (MD) simulations, the practical timescales of simulations are relatively short (10-100 ns). Of special interest in this work are MD simulations of systems with 'rugged' potential energy surfaces, which are characterized by numerous local (metastable) minima separated by high energetic barriers. Due to the limited timescales of MD simulations, simulations of such systems can suffer from inadequate sampling because they are trapped in these local minima. One common method to enhance the sampling of phase space is simulated annealing. In simulated annealing simulations, a system is given an initially high temperature, allowing it to overcome high energy barriers, and then gradually cooled to the desired temperature[2]. The simulated annealing technique is guaranteed to reach the global optimum of a system as the time taken to cool the system approaches infinity[3]. However, actual MD simulations cannot be infinite in length. During simulated annealing simulations, the system can become trapped in local energy minimum, escape from which is unlikely as the system is further cooled. The extent to which this occurs is specific to the system being simulated. Examples of a simulated annealing simulations using linear and stepped cooling are shown in Fig 1.1.

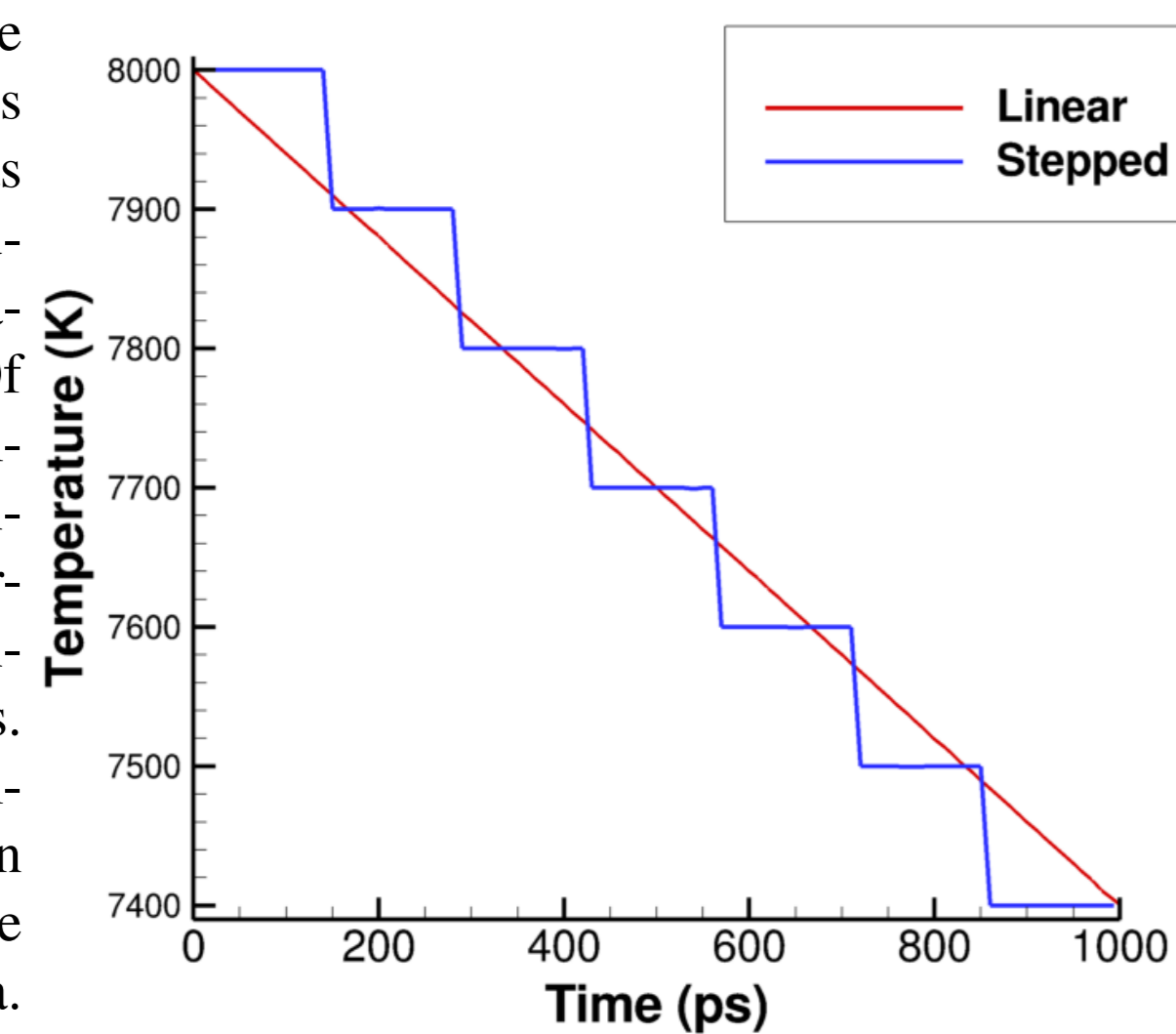


Figure 1.1: Simulated Annealing

1.2 Parallel Tempering

The goal of parallel tempering (or replica exchange) MD simulations is to increase the efficiency of the sampling of the phase space of a system. In parallel tempering molecular dynamics simulations, several replicas of a system are simulated independently and simultaneously at different temperatures[4]. At specified intervals, replicas with neighboring temperatures are exchanged with the Boltzmann weighted metropolis criterion:

$$P_{swap(i,j)} = \min(1, e^{(\beta_j - \beta_i)(U_i - U_j)}) \quad (1)$$

The random walk in temperature allows systems trapped in metastable states to escape by exchanging replicas with systems at higher temperatures. Systems at high temperatures are able to efficiently overcome large potential barriers, while systems at low temperatures selectively gain access to low energy structures. An advantage of parallel tempering simulations over simulated annealing is that exchange between low and high temperatures is possible throughout the entire simulation. However, one drawback to parallel tempering is the large number of replicas needed to cover the desired temperature interval. Efficient exchanges between replicas can only take place if there is some overlap between the potential energy of neighboring replicas over the course of a simulation. It has been shown that the number of replicas needed in a parallel tempering simulations scales approximately with the square root of the number of particles[5]. Additionally, simulations with a large number of replicas require increased simulation times for replicas to 'diffuse' over the range of temperatures and effectively cross barriers. An example of a parallel tempering simulation is shown in Fig. 1.2.

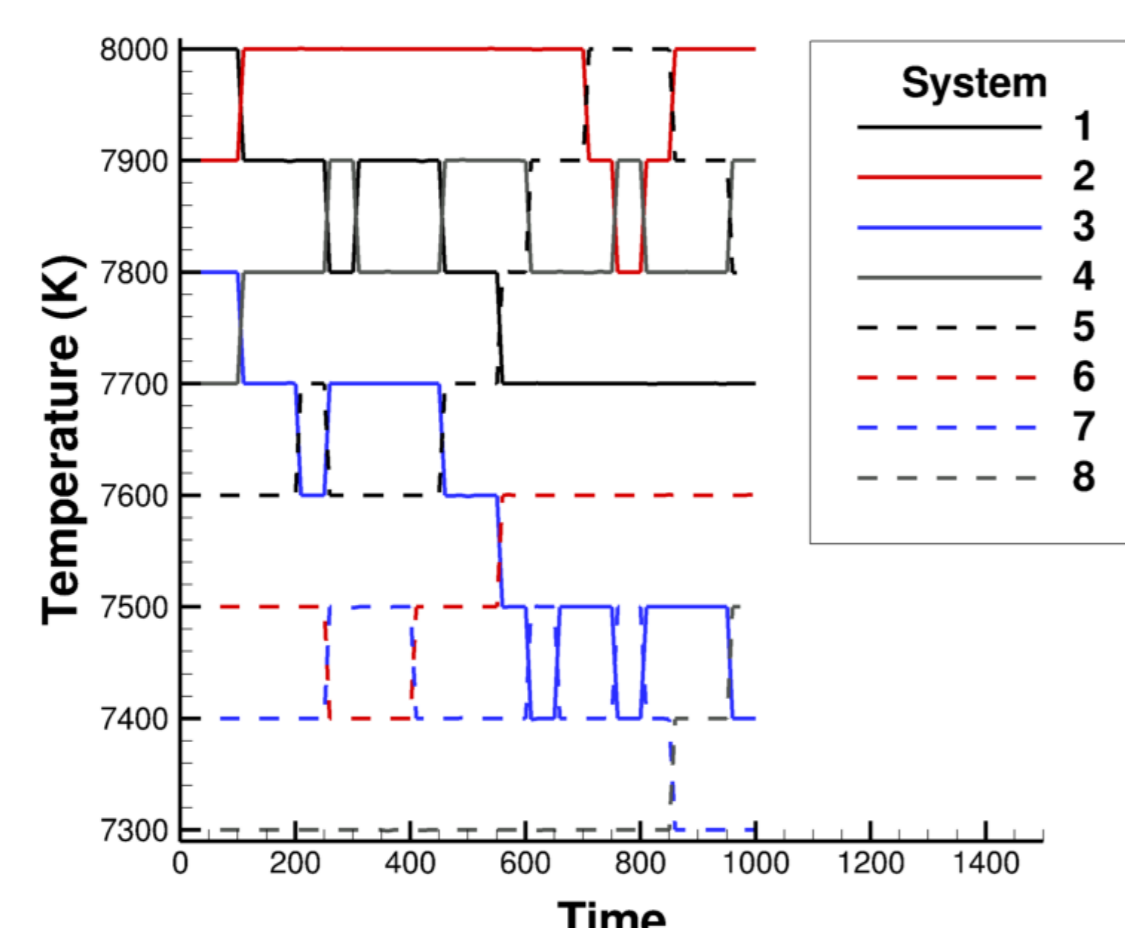


Figure 1.2 Parallel Tempering

1.3 Simulated Annealing combined with Parallel Tempering

By combining simulated annealing with parallel tempering, a method that shares the advantages of both techniques is created[6]. A small set of replicas are given a temperature distribution around a high temperature, and simulated via parallel tempering. At specified time intervals, each replica is cooled to a lower temperature, until the replicas are at the desired final temperature. This method keeps the efficient sampling of parallel tempering while relaxing the constraints on the large number of replicas needed. It has been shown to be more computationally efficient than simulated annealing for simulations of protein model structures, and requires fewer replicas than parallel tempering[6]. However, to fully realize the benefits of parallel tempering there must be a sufficient number of replica exchanges between temperature shifts, placing an upper bound on the cooling rate of the simulated annealing. An example of a simulation using simulated annealing combined with parallel tempering is shown in Fig. 1.3.

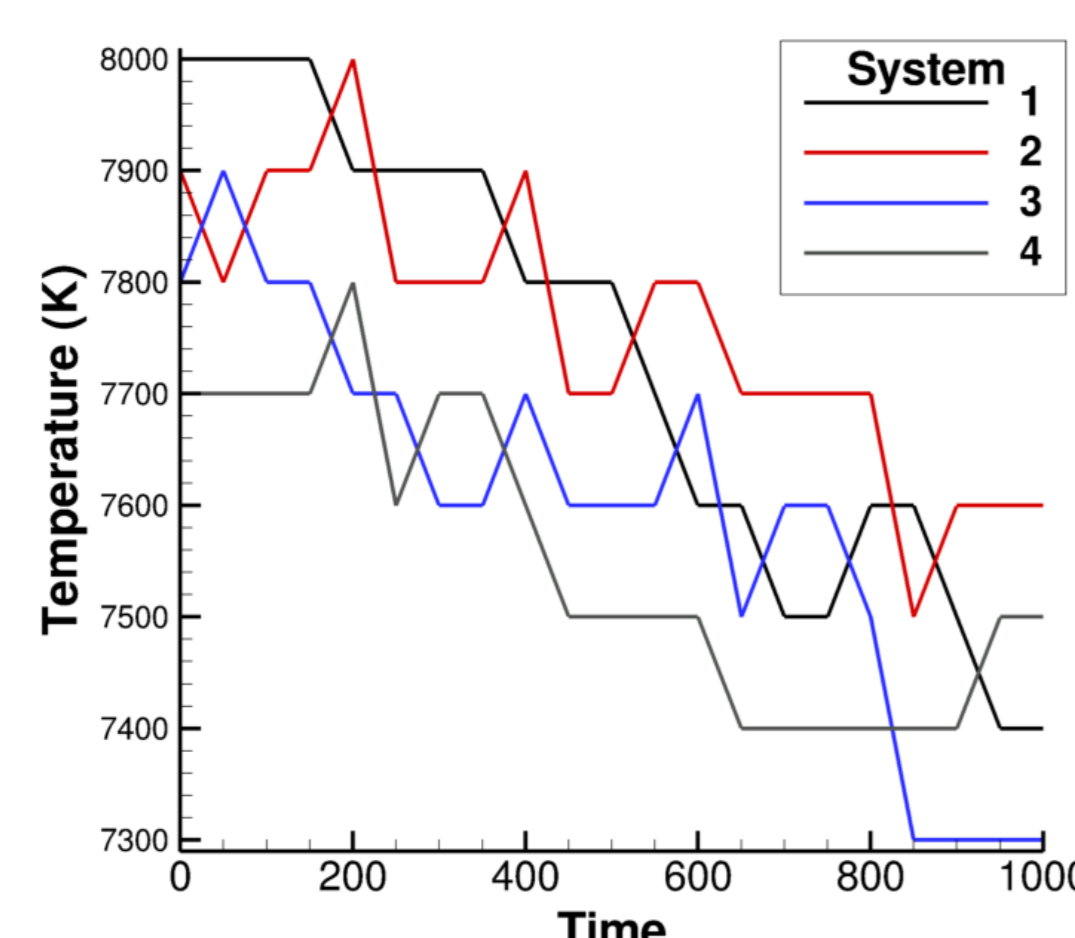


Fig 1.3: Simulated Annealing combined with Parallel Tempering

1.4 Implementation in LAMMPS

The capability to run both simulated annealing and parallel tempering simulations already exists in LAMMPS. Simulated annealing combined with parallel tempering was implemented in LAMMPS, and can be executed with the `anneal_temper` command in a typical input script. To run simulations the following syntax is used:

`anneal_temper N X Y W fix-ID seed1 seed2 T1 T2 T3 ... TN`

- N = Total number of timesteps to run
- X = Attempt tempering swap every this many steps
- Y = Shift temperature of T_i to T_{i+1} every this many steps
- W = Which entry on the temperature list (T₁ T₂ T₃ ... T_N) I am in simulations
- ID of the fix that will control temperature during the run
- seed1 = random number seed used to decide on adjacent temperature to partner with
- seed2 = random number seed for Boltzmann factor in Metropolis swap
- T₁ T₂ T₃ ... T_N List of temperatures to descend through.

The number of timesteps between temperature shifts (Y) must be a multiple of the number of timesteps between attempted swaps (X). If any individual world has a temperature of T_n, no more temperature shifts will occur. The method was validated by checking that it reproduced typical parallel tempering simulations before shifting occurred, and that it reproduced typical simulated annealing simulations when no swaps were allowed.

2 Application

2.1 Amorphous Silica Surfaces

We will consider the application of simulated annealing and simulated annealing with parallel tempering to dry amorphous silica surfaces. Amorphous silica (a-SiO₂) surfaces can be created by simply cleaving bulk a-SiO₂ along a desired plane. However, this creates an unrealistic surface covered with highly reactive broken bonds that could only be produced experimentally with infinitely high strain rates. Simulated annealing has previously been applied to a-SiO₂ surfaces to create more realistic surfaces[7]. Previous annealing simulations of a-SiO₂ surfaces have shown that short annealing simulations tend to leave a surface covered with more defects, while longer simulations annealing simulations decrease number of defects on the surface[8]. Experimental evidence suggests that real a-SiO₂ surfaces annealed over long timescales (hours) have very few defects and are primarily terminated with bridging oxygen atoms (Si-O-Si)[9]. Our goal is to approach realistic, defect free surfaces by accelerating annealing simulations with parallel tempering. Realistic a-SiO₂ surfaces are important for numerous applications, including simulations of the chemical reaction occurring on silica heat shields during reentry[8].

Typical annealing simulations of a-SiO₂ surfaces have a temperature range from 4000 K - 300 K[7]. To run parallel tempering simulations, it is necessary to create a list of temperatures spanning this range. These temperatures must be chosen such that there is a reasonable swapping probability between replicas. It has been shown that for parallel tempering simulations of model proteins that a swapping probability of 20-40% is desirable[6].

For the purpose of our simulations, we will use a 20 Å x 35 Å x 35 Å slab of a-SiO₂ (~1600 atoms), created by cleaving a previously annealed bulk along the (001) plane. For all simulations we will use the the BKS interatomic potential[10] with the modifications suggested by Jee et al.[11]. To check how the swapping probability varies with the temperature difference, we ran parallel tempering simulations with two replicas. A total of 200 exchanges were attempted with a frequency of 1 attempt/ps. In all cases the temperature of the higher replica was 4000 K. As shown in Fig. 2.1, the exchange probability decreases with the temperature difference. For simulations with this slab, we will use ΔT= 50 K at 4000 K, which corresponds to a swapping probability of ~20%. The list of temperatures used in the simulated annealing with parallel tempering simulations is generated with the equation:

$$T_i = Ae^{k \cdot i} \quad (2)$$

The exchange probability between replicas remains constant over the temperature list created by this equation. Using the parameters A = 1000 K and k = 0.011, this produces a list of 128 temperatures between 4000 K - 1000 K, with ΔT = 50K near 4000 K. A parallel tempering simulation using this temperature list would require 128 individual replicas.

The three additional parameters that are needed for simulations are: the time between swap attempts, the time between temperature shifts, and the number of local replicas. The time between swap attempts must be large enough that replicas undergo appreciable conformational changes between exchange attempts. Figure. 2.1 shows the mean square displacement of atoms in the slab at different temperatures. It might be optimal to adjust the shift attempt frequency with temperature so it corresponds directly to a constant value of mean square displacement, however this goes beyond the capabilities of current implementation of the method. We will attempt temperature swaps every 1 ps, which gives a mean square diffusion of about 1 Å per swap attempt at 4000 K. The number of replicas used must be large enough to span a temperature range that allows replicas to overcome whatever potential barriers exist in the system, and the time between shifts must allow sufficient time for individual replicas to overcome these barriers via exchange. We will use four local replicas, which span as much as 175 K in temperature, and perform temperature shifts every 10 ps.

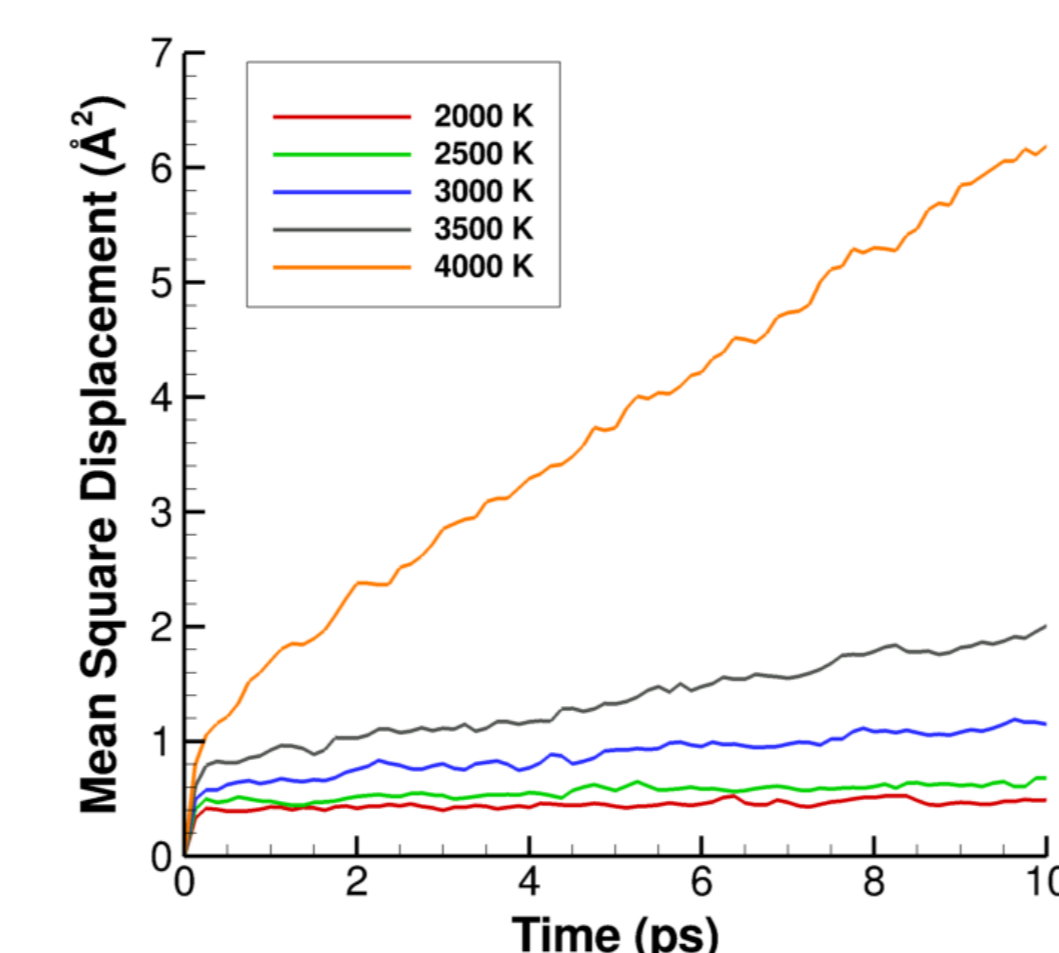


Fig 2.1: Swapping Probability vs. T

Fig 2.2: MSD vs. T

2.2 Results And Discussion

We will compare the results of simulated annealing to simulated annealing with parallel tempering. To perform a relevant comparison, simulated annealing simulations are run with a linear cooling schedule with the same temperature list as simulated annealing with parallel tempering simulations. Four pairs of simulations were run, each with different starting a-SiO₂ surfaces cleaved from the bulk. We will use two metrics to determine the efficacy of the techniques: surface energy and defect concentration. The surface energy is defined as the difference between the energy of the slab exposed to vacuum and the energy of the slab in the bulk, divided by area of the slab. There are several types of defects predicted by the BKS potential on a-SiO₂ surfaces: under-coordinated silicon atoms (≡Si· as shown in Fig. 2.2(b)), non-bridging oxygen (≡Si-O· and =Si-O·, as shown in Fig. 2.2(c) and (d) respectively), and Si₂O₂ rings (shown in Fig 2.2(e)). These defects can be uniquely identified by their connectivity to other atoms in the slab. An annealed a-SiO₂ surface with ≡Si· defects highlighted is shown in Fig. 2.2(a).

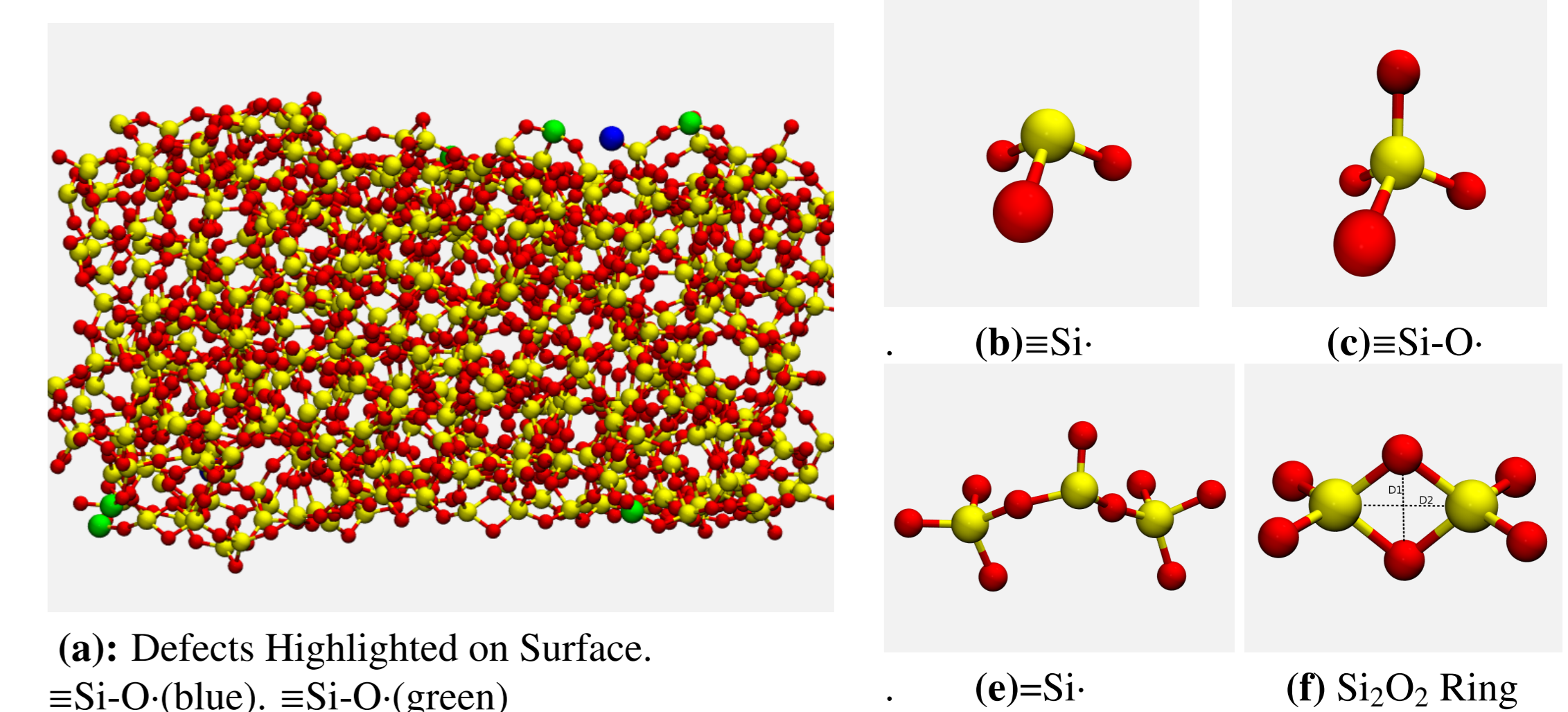


Fig 2.2: a-SiO₂ Surface with Defects

Method	Defect Concentration (1/Å ²)					Surface Energy (meV/Å ²)
	Total	Si ₂ O ₂	≡Si·	≡Si-O·	=Si-O·	
Parallel Tempering with Simulated Annealing	0.726	0.552	0.112	0.127	0.008	18.89
Simulated Annealing	0.7811	0.482	0.165	0.132	0.002	21.7
Simulated Annealing (2x slower)	0.676	0.388	0.149	0.129	0.009	19.2

Table 1: Comparison of a-SiO₂ Surfaces created with different methods

As shown in Table 1 the surfaces created by simulated annealing with parallel tempering are slightly fewer defects and slightly lower surface energies than those created with simulated annealing. An additional simulated annealing simulation run at half the cooling rate (and thus twice the CPU time) creates a surfaces with fewer defects but a higher surface energy than simulated annealing with parallel tempering. These results demonstrate that simulated annealing with parallel tempering is faster than simulated annealing alone for this system, and even has the potential to be more efficient in terms of total CPU time used. It has been shown that this method, when finely tuned for certain systems, can be more efficient than simulated annealing alone[6]. However, additional annealing simulations would need to be needed to confirm this.

3 Conclusions

The hybrid method of simulated annealing with parallel tempering was implemented in LAMMPS. This method shares the advantages of simulated annealing and parallel tempering, and uses fewer replicas than parallel tempering alone. We applied this method to a-SiO₂ silica surfaces and found that it was more effective than simulated annealing at creating low-defect surfaces. However, to successfully apply this method to a general system, care must be taken in choosing the parameters to suit the specific needs of the system. The primary limitation of this method is that as the total number of atoms in a system increases, the maximum cooling rate decreases. This method would be most effective when applied to smaller systems of atoms, or simulations with computationally expensive interatomic potentials.

REFERENCES

- [1] Plimpton, S., "Fast Parallel Algorithms for Short-Range Molecular Dynamics," *J. Computational Physics*, Vol. 117, 1995, pp. 1-19, lammps.sandia.gov.
- [2] Kirkpatrick, S., C.D. Gelatt, J., and Vecchi, M. P., "Optimization by Simulated Annealing," *Science*, Vol. 220, No. 4598, 1983.
- [3] Mitra, D., Romeo, F., and Sangiovanni-Vincentelli, A., "Convergence and Finite-Time Behavior of Simulated Annealing," *Advanced Applied Probability*, Vol. 18, 1986, pp. 747-771.
- [4] Fukunishi, H., Watanabe, O., and Takda, S., "On the Hamiltonian replica exchange method for efficient sampling of biomolecular systems: application to protein structure prediction," *Journal of Chemical Physics*, Vol. 116, 2002, pp. 9058-9067.
- [5] Tathore, N., Chopra, M., and de Pablo, J., "Optimal allocation of replicas in parallel tempering simulations," *Journal of Chemical Physics*, Vol. 122, 2005.
- [6] Kannan, S. and Zacharias, M., "Simulated annealing coupled replica exchange molecular dynamics - An efficient conformational sampling method," *Journal of Structural Biology*, 2009, pp. 288-294.
- [7] Fogarty, J., Aktulga, H., Grama, A., and van Duin, A., "A reactive molecular dynamics simulation of the silica water interface," *The Journal of Chemical Physics*, Vol. 132, 2010, pp. 174704.
- [8] Norman, P., Schwartzentruber, T., and Cozmuta, I., "A computational Chemistry Methodology for Developing an Oxygen-Silica Finite Rate Catalytic Model for Hypersonic Flows," *42nd AIAA Thermophysics Conference, Honolulu, Hawaii, June 27-30, 2011*.
- [9] Sneh, O. and George, S., "Thermal Stability of Hydroxyl Groups on a Well-Defined Silica Surface," *The Journal of Chemical Physics*, 1995, pp. 4639-4647.
- [10] Beest, B., Kramer, G., and van Santen, R., "Force Fields for Silicas and Aluminophosphates Based on Ab Initio Calculations," *Physical Review Letters*, Vol. 64, No. 16, 1990.
- [11] Jee, S., McGaughey, A., and Sholl, D., "Molecular simulations of hydrogen and methane permeation through pore modified zeolite membranes," *Molecular Simulation*, Vol. 35, 2009.